sciendo

Optoelectronics applications of electrodeposited p- and n-type Al$_2$Se$_3$ thin films

A. A. Faremi[1,*], S. S. Oluyamo[2], O. Olubosede[1], I. O. Olusola[2], M. A. Adekoya[3], A. T. Akindadelo[4]

[1]Department of Physics, Federal University Oye-Ekiti, Ekiti State, Nigeria

[2]Condensed Matter and Statistical Physics Research Unit, Department of Physics, School of Sciences, The Federal University of Technology, Akure, Nigeria

[3]Department of Physics, Edo University Iyamho, Auchi, Edo State, Nigeria

[4]Basic Sciences Department, Physics/Electronics Unit, Babcock University, Ilisan-Remo, Ogun State, Nigeria

In this paper, energy band gaps and electrical conductivity based on aluminum selenide (Al$_2$Se$_3$) thin films are synthesized electrochemically using cathodic deposition technique, with graphite and carbon as cathode and anode, respectively. Synthesis is done at 353 K from an aqueous solution of analytical grade selenium dioxide (SeO$_2$), and aluminum chloride (AlCl$_2$·7H$_2$O). Junctions-based Al$_2$Se$_3$ thin films from a controlled medium of pH 2.0 are deposited on fluorine-doped tin oxide (FTO) substrate using potential voltages varying from 1,000 mV to 1,400 mV and 3 minutes -15 minutes respectively. The films were characterized for optical properties and electrical conductivity using UV-vis and photoelectrochemical cells (PEC) spectroscopy. The PEC reveals a transition in the conduction of the films from p-type to n-type as the potential voltage varies. The energy band gap reduces from 3.2 eV to 2.9 eV with an increase in voltage and 3.3 eV to 2.7 eV with increase in time. These variations indicate successful fabrication of junction-based Al$_2$Se$_3$ thin films with noticeable transition in the conductivity type and energy band gap of the materials. Consequently, the fabricated Al$_2$Se$_3$ can find useful applications in optoelectronic devices.

Keywords: *electrodeposition, cathodic graphide, p- and n-type Al$_2$Se$_3$, energy gap*

1. Introduction

In recent times, compound semiconductor materials, such as cadmium telluride (CdTe), zinc oxide (ZnO), zinc sulfide (ZnS), lead sulfide (PbS), aluminum selenide (Al$_2$Se$_3$), and cadmium selenide (CdSe) to mention a few, have experienced renewed scientific attention as they form the bedrock of many scalable technologies [1]. Among the compound semiconductors, aluminum selenide (Al$_2$Se$_3$) thin films are the most infrequently described despite their potential in optoelectronic applications [2]. Aluminum (Al) as an elemental semiconductor has been extensively studied because of its ease of growth, promising optical and electrical properties, and abundance in the earth's crust, after oxygen and silicon [2–4]. Although compound semiconductor has more

functionalities than elemental semiconductor [5–7], compound semiconductors also possess more functionalities than their respective components. In addition, compound semiconductors with selenium as a constituent portend viable nanomaterials in energy conversion solar cells and sensor devices [2, 8–10]. Al$_2$Se$_3$ has also been described as a perfect window layer material that is capable of forming a suitable heterojunction with absorber layer materials such as cadmium telluride and lead sulfide. The suitability of this material in the formation of heterostructure-based optoelectronic devices necessitate the study of junction-based Al$_2$Se$_3$. Compound semiconductor materials based thin films have been synthesized by various deposition techniques [11–13]. Among all the synthesis routes, the electrodeposition (ED) technique plays a significant role in the synthesis of cost-effective nanomaterials for nanodevice applications [14–17]. This method allows tunability and

---

*E-mail: abass.faremi@fuoye.edu.ng

control of nanomaterials' properties by changing the preparative parameters of the solution, such as ionic concentration (electrolyte), pH value, temperature, deposition time, and cathodic voltage [18–20].

To our knowledge, researchers over the years have paid little to no attention to the electrical conduction type of Al_2Se_3, especially when the cathodic potential varies. In this work, the focus is directed toward the possibility of fabrication of both p-and n-type Al_2Se_3 without the inclusion of external dopants. It is believed that most nanodevices are p-n junction-based devices; therefore n-type and p-type Al_2Se_3 will be of commercial value in the fabrication of single material-based junction devices such as diodes.

2. Material and method

The film of Al_2Se_3 sourced from the solution of high-grade aluminum chloride ($AlCl_2$, 99%) and selenium dioxide (SeO_2, 99%) without further purification were subject to ED on a thoroughly degreased conducting fluorine-doped tin oxide (FTO)/substrate of 2.3 by 4 cm^2 dimension. The formation of electrolytic bath of Al_2Se_3 contained 29 g of $AlCl_2$ and 0.9 g of SeO_2. The admixed solution of 400 mL in a 500 mL beaker was magnetically stirred for 2 h to ensure homogeneous solution and the acidic level was tested and adjusted using both pH probe (pH = 2.5) and ammonium solution, since the synthesis technique used is favored by acidic medium [20]. Different films of Al_2Se_3 at a bath temperature of 90 °C in 15 min were achieved potentiostatically in two-electrode configurations; graphite was used as a counter electrode (cathode) and carbon as a reference electrode (anode) by the variation of cathodic potential and duration of deposition, respectively. The film's optical properties and electrical conductivity type were achieved using ultraviolet-visible spectroscopy at wavelength range 200–900 nm and photoelectrochemical cells (PEC) measurements. Thin-film thickness, optical properties, and electrical conductivity type were obtained using Eqs (1)–(4) [21, 22].

$$T = \frac{JtM}{\rho nF} \tag{1}$$

The film thickness as illustrated in Table 1 is denoted as T, J is the current density of the electrodeposited Al_2Se_3, t is the deposition time, ρ is the density of Al_2Se_3, n is the total number of electrons transferred per ion of the deposited material, F is the faraday's constant with a numerical value of 96,485 $C \cdot mol^{-1}$, and M is the molar weight of the deposited Al_2Se_3.

$$(\alpha h\nu) = A (h\nu - E_g)^n \tag{2}$$

where α is absorption coefficient, $h\nu$ is photon energy, A is a constant usually equal to one, E_g is the energy band gap, and n is the transition between the valence band and conduction band, which is 0.5 for direct and 1 for indirect transition.

$$k = \frac{\alpha\lambda}{4\pi} = \frac{\alpha\lambda}{12.57} \tag{3}$$

where α is absorption coefficient, k is extinction coefficient, and 4π carries a numeric value of 12.57.

$$PEC\ Signal = V_L - V_D \tag{4}$$

where V_L is voltage under illumination and V_D is voltage under dark.

3. Results and discussion

3.1. Optical properties of junction-based electrodeposited Al_2Se_3

The optical properties of the electrodeposited aluminum selenide as a function of optimized time of deposition and cathodic potential are shown in Figures 1–4. From Figure 1, it can be seen that material energy band gaps are not only dependent on films' thickness but also a function of preparative parameters, as there is a noticeable decrease in the energy band gap as time (3.30–2.70 eV) and voltage (3.23–2.95 eV) increase. The energy bang gaps

values obtained as both time and voltage increase are determined by the extrapolation of the linear part of the energy band gap graphs. The changes in the film's bandgap are a result of optical properties' dependence on particle dimension, causing the quantum conferment effect [13]. However, such preparative parameters reveal significant improvement in the built-in electric field, as the slope of the energy band diagram is well defined [19, 23]. The absorbance spectra of Al$_2$Se$_3$ thin films deposited at varied times and voltage as depicted in Figure 4 clearly showed a decrease in the absorbance with an increase in the wavelength. From Figure 2, two absorption bands are observed. The first absorption band (Figure 2(A)) is an indication of Al$_2$Se$_3$ band edge peak close to quantum dot in the visible region that indicates blue shift [3]. The second absorption band, as shown in Figure 2(B), revealed maximum absorption in the infrared region of the spectrum, which suggests that the film is a good radiation detection material [24]. The absorption characteristic revealed the suitability of Al$_2$Se$_3$ as a good buffer/window material in optoelectronics applications. Figure 3 reveals the transmittance characteristic of the film as a function of wavelength, time of deposition, and cathodic potential. High transmittance peaks as observed in Figure 3(A and B), with values >80%, make the films a good receptive surface to any absorber layer [25]. There is a reflection of radiation light in the films as depicted in Figure 4, which is an indication that reflection of light occurs within the electromagnetic region. Such transition in reflectance revealed the potential of the films as good anti-reflection coating suitable for optoelectronic applications.

3.2. Optical constant of junction-based electrodeposited Al$_2$Se$_3$

Figures 5 and 6 showed that there is a relatively low absorption edge within the visible region. However, a good absorption edge was observed in the film deposited at various cathodic potentials, which suggests a variation of cathodic potential as a good preparative procedure in the fabrication of optoelectronics materials using the ED technique. The Al$_2$Se$_3$ layers grown at varied ca-
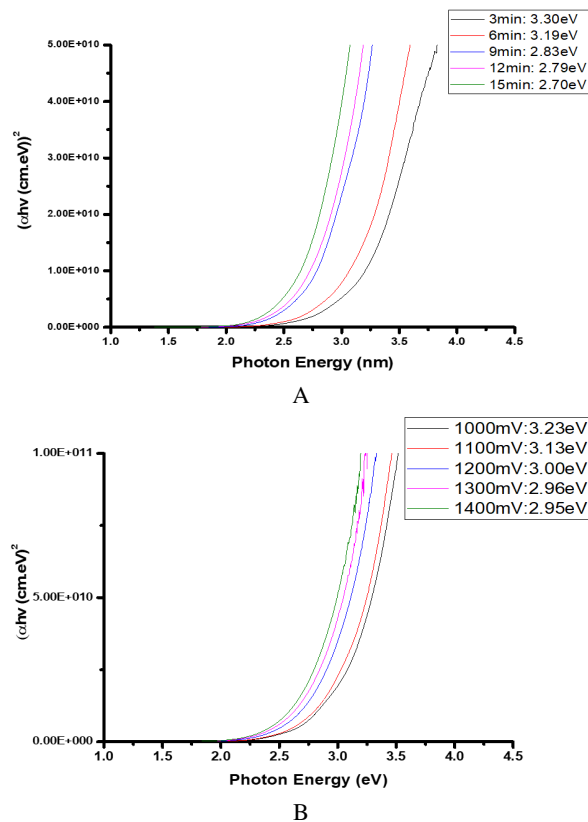
Fig. 1. The energy band gap of Al$_2$Se$_3$ at varied (A) time of deposition and (B) cathodic potential.

thodic potentials and times of deposition, respectively, have the highest extinction values within the visible to the near-infrared wavelength region.

3.3. Electrical conductivity type of electrodeposited Al$_2$Se$_3$

To ascertain the conductivity type of electrodeposited aluminum selenide and suggest possible preparative parameters to the realization of semiconductor type, a PEC measurement was carried out, which was achieved by forming a liquid junction between the substrate and the electrolyte. Figure 7(A) shows the electrical conductivity type span with the negative region, despite the variation in deposition time resulting in n-type material. The PEC signal, measured under conditions of darkness and illumination as depicted in Figure 7(B), revealed the transition from p-type to n-type. At low cathodic voltages, the PEC signal falls within the positive region indicating p-type Al$_2$Se$_3$.
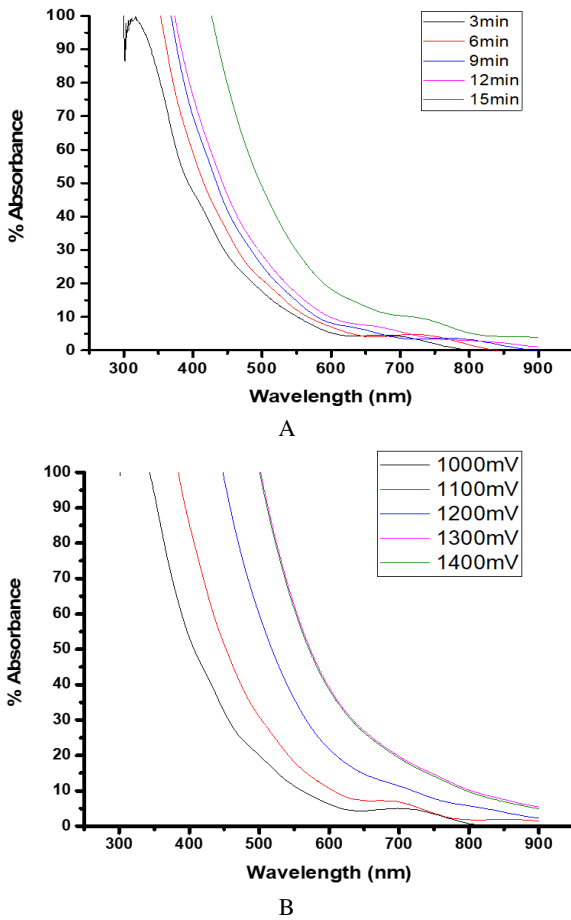
Fig. 2. Absorption spectra as a function of wavelength at varied (A) time and (B) voltage (B).
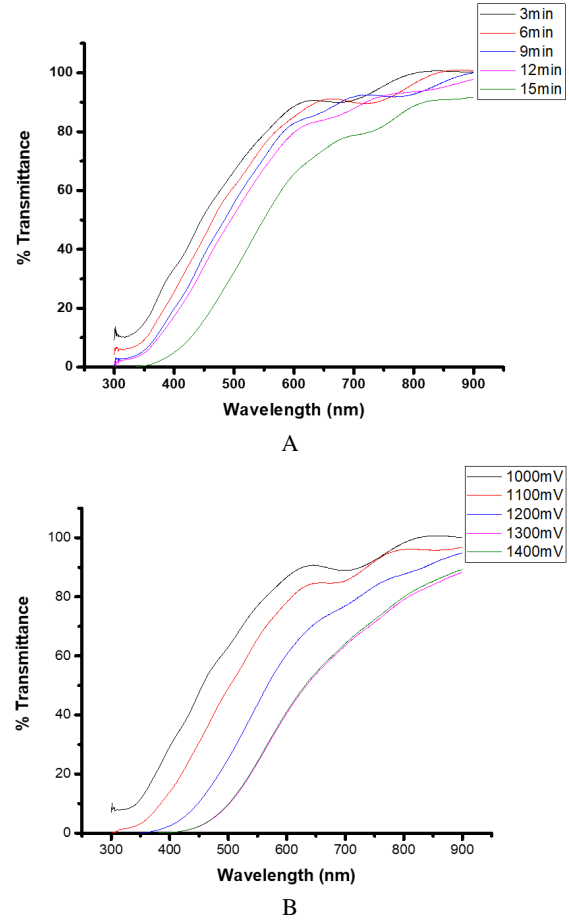
Fig. 3. Percentage of transmittance of Al_2Se_3 as a function of wavelength at varied (A) time and (B) voltage.

As the cathodic voltages increased >1,100 mV, the PEC signal transited to the negative region showing n-type Al_2Se_3. However, one can conclude that the film's conductivity type transition depends only on the variation of growth voltage and not on the time of deposition (Table 2). Our observation affirms that the film electrical conductivity type cannot be tuned under the influence of time variation but requires post-heat-treatment in accordance with previous researches [17, 23, 25–27].

4. Conclusion

The achievement of junction-based electrodeposited aluminum selenide revealed the potential of the films in optoelectronics applications. The result obtained in the optical phenomena and constants

Table 1. Measured material properties as a function of deposition time and cathodic potential based on UV and PEC results.

Semiconductor type and energy band gaps					
As time of deposition increases			As voltage increases		
Time (min)	Type	Eg (eV)	Cathodic potential (mV)	Type	Eg (eV)
3	N	3.30	1,000	P	3.23
6	N	3.19	1,100	I-Intrinsic	3.20
9	N	2.83	1,200	N	3.00
12	N	2.79	1,300	N	2.96
15	N	2.70	1,400	N	2.95

PEC, photoelectrochemical cells.

Table 2. Film thickness values with the variation in the time of deposition and cathodic potential.

Film thickness as the time of deposition increases		Film thickness as the cathodic potential increases	
Time (min)	Thickness (nm)	Cathodic potential (mV)	Thickness (nm)
3	193	1,000	234
6	233	1,100	344
9	399	1,200	522
12	476	1,300	714
15	592	1,400	773
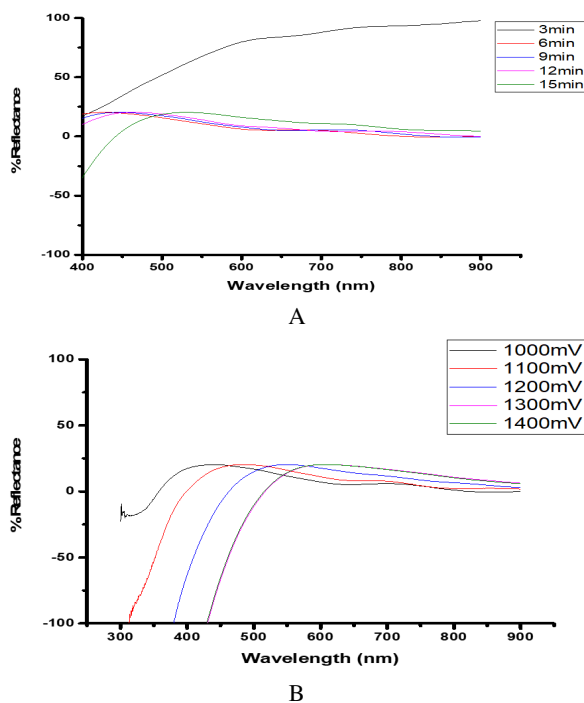
Fig. 4. Reflection spectra as a function of wavelength at varied (A) time and (B) voltage.

Fig. 5. Absorption coefficient as a function of wavelength at varied (A) time and (B) voltage.

suggests cathodic potential and time of deposition as good preparative parameters in the tunability of optical properties of electrodeposited Al$_2$Se$_3$ thin films. The film energy bandgap varied from 3.23 eV to 2.95 eV as cathodic voltage increases, and from 3.3 eV to 2.7 eV as the time of deposition increases, respectively. The other optical properties with relatively low absorbance, averagely high reflectance, and high transmittance indicate the viability of junction-based electrodeposited Al$_2$Se$_3$ as good buffer/window layers in solar cell device architecture. The absorption and extinction coeffi- cient showed a sharper absorption edge and higher extinction coefficient edge in the visible region of the electromagnetic spectrum. The films possess excellent optical constant, which helps in the selection of good window layer materials capable of providing a receptive surface for absorber layers in the fabrication of junction-based optoelectronics devices. The successful fabrication of p-type and
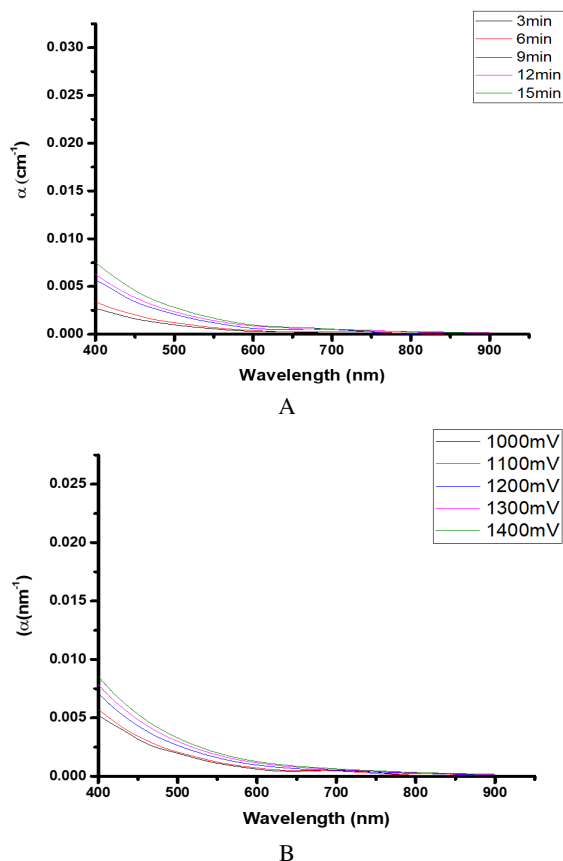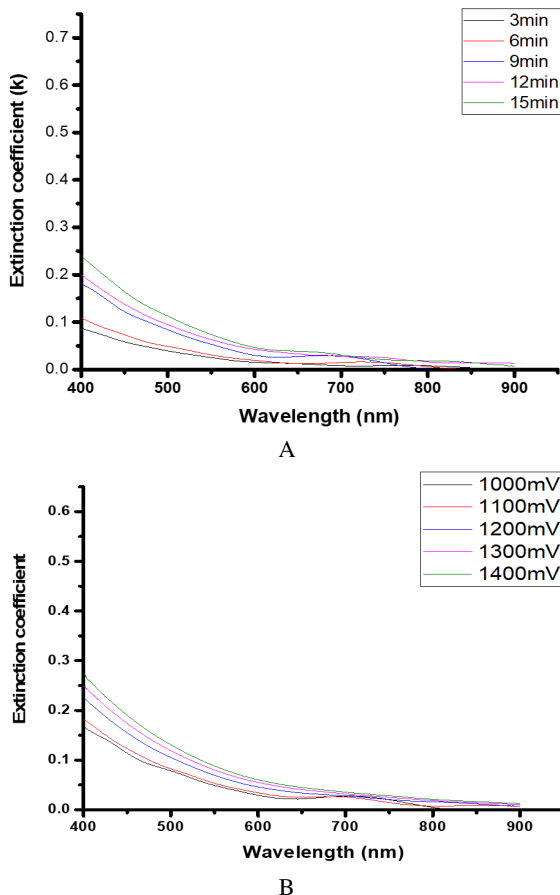
Fig. 6. Extinction coefficient as a function of wavelength at varied (A) time and (B) voltage.

Fig. 7. PEC signal as a function of growth voltage for glass/FTO/Al$_2$Se$_3$ layers at varied (A) time and (B) voltage. FTO, fluorine-doped tin oxide; PEC, photoelectrochemical cells.

n-type Al$_2$Se$_3$ suggests cathodic potential as an optimized preparative procedure in the ED technique.

Acknowledgement

References

[1] Huang KC, Liu CL, Hung PK, Houng MP. Cyclic voltammetric study and nucleation of electrodeposited Cu(In,Al)Se2 thin films with sodium dodecyl sulfate additive. J Electrochem Soc. 2013; 160(4):D125–D131; https://doi.org/10.1149/2.029304jes

[2] Adams JA, Bostwick A, Ohta T, Ohuchi FS, Olmstead MA. Heterointerface formation of aluminum selenide with silicon: Electronic and atomic structure of Si(111): AlSe. Phys Rev B. 2005;71(19):1–8; https://doi.org/10.1103/PhysRevB.71.195308

[3] Balitskii OA, Demchenko PY, Mijowska E, Cendrowski K. Synthesis and characterization of luminescent aluminium selenide nanocrystals. Mater Res Bull. 2013; 48(2):916–9; https://doi.org/10.1016/j.materresbull.2012.11.059

[4] Beck G, Funk S. Correlation between optical appearance and orientation of aluminium. Surf Coat Technol. 2012; 206(8–9):2371–9; https://doi.org/10.1016/j.surfcoat.2011.10.034

[5] Lincot D. Electrodeposition of semiconductors. Thin Solid Films. 2005; 487(1–2):40–8; https://doi.org/10.1016/j.tsf.2005.01.032

[6] Wang Y, Zhong K, Zhang N, Kang Y. Numerical analysis of solar radiation effects on flow patterns in street canyons. Eng Appl Comput Fluid Mech. 2014; 8(2):252–62; https://doi.org/10.1080/19942060.2014.11015511

[7] Asaduzzaman M, Bahar AN, Bhuiyan MMR, Habib MA. Impacts of temperature on the performance of CdTe based thin-film solar cell. IOP Conf Ser Mater Sci Eng. 2017; 225(1):012274; https://doi.org/10.1088/1757-899X/225/1/012274

[8] Ikhioya IL, Ijabor BO, Whyte GM, Ezema FI. Synthe-

sis and characterization of aluminium sulphide (Al2S3) thin films. Chem Methodol. 2019; 3(6):715–6; `https://doi.org/10.33945/sami/chemm.2019.6.4`

[9] Shavel A, Gaponik N, Eychmu A. Efficient UV-blue photoluminescing thiol-stabilized water-soluble alloyed ZnSe (S) nanocrystals. J Phys Chem B. 2004;108(19):5905–8.

[10] Min HS. Characterization of N-Type and P-Type thin films. Chem Sci J. 2016; 7(2):4172; `https://doi.org/10.4172/2150-3494.1000e113`

[11] Chaudhari JB, Deshpande NG, Gudage YG, Ghosh A, Huse VB, Sharma R. Studies on growth and characterization of ternary CdS 1-xSex alloy thin films deposited by chemical bath deposition technique. Appl Surf Sci. 2008; 254(21):6810–6; `https://doi.org/10.1016/j.apsusc.2008.04.081`

[12] Chaudhari KB, Gosavi NM, Deshpande NG, Gosavi SR. Journal of science : Advanced materials and devices chemical synthesis and characterization of CdSe thin films deposited by SILAR technique for optoelectronic applications. J Sci Adv Mater Devices. 2016; 1(4):476–1; `https://doi.org/10.1016/j.jsamd.2016.11.001`

[13] Echendu OK, Dharmadasa IM. Graded-bandgap solar cells using all-electrodeposited ZnS, CdS and CdTe thin-films. Energies. 2015;8(5):4416–35; `https://doi.org/10.3390/en8054416`

[14] Raffaelle RP, Mantovani JG, Bailey SG, Hepp AF, Gordon EM, Haraway R. Electrodeposited CuInSe2 thin film junctions. NASA Conf Publ. 1998; 208413:47; `https://doi.org/10.1557/PROC-495-383`

[15] Strauss AJ, The AJS, Appliquee DP. The physical properties of cadmium telluride. Revue de Physique Appliquee. 1977;12(2):167–84.

[16] Mahalingam T, John VS, Rajendran S, Sebastian PJ. Electrochemical deposition of ZnTe thin films. Semicond Sci Technol. 2002; 17(5):465–70; `https://doi.org/10.1088/0268-1242/17/5/310`

[17] Dharmadasa IM, Madugu ML, Olusola DI, Echendu OK, Fauzi F, Diso DG, et al. Electroplating of CdTe thin films from cadmium sulphate precursor and comparison of layers grown by 3-electrode and 2-electrode systems. Coatings. 2017; 7(2):17; `https://doi.org/10.3390/coatings7020017`

[18] Diso DG, Fauzi F, Echendu OK, Olusola OI, Dharmadasa IM. Optimisation of CdTe electrodeposition voltage for development of CdS/CdTe solar cells. J Mater Sci Mater Electron. 2016;27(12):12464–72; `https://doi.org/10.1007/s10854-016-4844-3`

[19] Samuel S, Akande A, Olusola OI, Adelaja Y. Materi-als Today : Proceedings Tunability of conductivity type and energy band gap of CdTe thin film in the electrodeposition technique. Mater Today Proc. 2020; `https://doi.org/10.1016/j.matpr.2020.02.962`

[20] Echendu OK, Okeoma KB, Oriaku CI, Dharmadasa IM. Electrochemical deposition of CdTe semiconductor thin films for solar cell application using two-electrode and three-electrode configurations: A comparative study. Adv Mater Sci Eng. 2016;2016:10–14; `https://doi.org/10.1155/2016/3581725`

[21] Slonopas A, Alijabbari N, Saltonstall C, Globus T, Norris P. Electrochimica acta chemically deposited nanocrystalline lead sulfide thin films with tunable properties for use in photovoltaics. Electrochim Acta. 2015;151:140–9; `https://doi.org/10.1016/j.electacta.2014.11.021`

[22] Kim J, Kim HT, Park C. Synthesis and characterization of cadmium telluride nanocrystals for using hybrid solar cell. Int Conf Opt MEMS Nanophotonics. 2011:227–228; `https://doi.org/10.1109/OMEMS.2011.6031101`

[23] Ojo AA, Dharmadasa IM. Electroplating of semiconductor materials for applications in large area electronics: A review. Coatings. 2018;8(8):262; `https://doi.org/10.3390/coatings8080262`

[24] Milbrath BD, Peurrung AJ, Bliss M, Weber WJ. Radiation detector materials: An overview. J Mater Res. 2008; 23(10):2561–81; `https://doi.org/10.1557/jmr.2008.0319`

[25] Olusola OI, Oluyamo SS, Ajayi OA. Materials science in semiconductor processing opto-electronic properties of electrodeposited ZnTe using zinc anode as counter electrode. Mater Sci Semicond Process. 2020:105494; `https://doi.org/10.1016/j.mssp.2020.105494`

[26] Kumarasinghe KD, De Silva DS, Pathiratne KA, Salim HI, Abdul-Manaf NA, Dharmadasa IM. Electrodeposition and characterization of as-deposited and annealed CdTe thin films. Ceylon J Sci. 2016;45(2):53; `https://doi.org/10.4038/cjs.v45i2.7388`

[27] Salim HI, Patel V, Abbas A, Walls JM, Dharmadasa IM. Electrodeposition of CdTe thin films using nitrate precursor for applications in solar cells. J Mater Sci Mater Electron. 2015;26(5):3119–28; `https://doi.org/10.1007/s10854-015-2805-x`